Adv. Geosci., 67, 15–24, 2025
https://doi.org/10.5194/adgeo-67-15-2025

Advances in Geosciences
Open Access
EGU

Preliminary laboratory studies on hydrogen storage in a salt cavern of the Eocene Barbastro Formation, Southern Pyrenees, Spain

Timea Kovács[1], José Mediato[1], Berta Ordóñez[1], Nuria Garcia-Mancha[2], Pablo Santolaria[5], Pablo Calvín[6], José Sanchez Guzman[3], Jesús Gracia[3], Sara Roces[1,4], Pilar Mata Campos[1,✞], and Edgar Berrezueta[1]

[1]Instituto Geológico y Minero de España (CN-IGME. CSIC), Oviedo, Spain, Spain
[2]Centro Nacional del Hidrógeno, Ciudad Real, Spain
[3]Salmueras Depuradas SL, Monzón, Spain
[4]Universidad de Oviedo, Oviedo, Spain
[5]Institut de Recerca Geomodels and Departament de Dinàmica de la Terra i de l'Oceà, UB (University of Barcelona), Barcelona, Spain
[6]Departamento de Geología, Universidad de Salamanca, Salamanca, Spain
✞deceased

Correspondence: Timea Kovács (t.kovacs@igme.es)

Received: 12 June 2025 – Revised: 7 August 2025 – Accepted: 19 August 2025 – Published: 10 October 2025

Abstract. Underground hydrogen storage (UHS) is emerging as a promising tool for managing surplus energy derived from renewable energy sources. Rock salt (halite) formations, particularly solution-mined salt caverns, offer a secure and efficient storage medium due to their low permeability, self-healing properties, and chemical stability. Laboratory experiments simulating reservoir-like conditions are essential for reducing uncertainties surrounding hydrogen–rock interactions prior to large-scale deployment. This study investigates the response of rock salt to hydrogen exposure under controlled conditions (10 MPa, 60 °C, 30 d) in an autoclave. Two samples from the Eocene Barbastro Formation (Southern Pyrenees), recovered from a deep borehole within a potential salt cavern-type storage site, were tested. The halite samples included impurities such as anhydrite, quartz, feldspars, dolomite, calcite, and phyllosilicates, allowing assessment of non-halite phase reactivity also. Results indicate no significant mineralogical changes after hydrogen exposure. Observed alterations were minor and limited to localised halite recrystallization, slight particle detachment, and occasional chloride precipitation. These findings suggest an overall mineralogical stability of the salt matrix and impurities under the tested conditions and scales. By improving our understanding of hydrogen–rock interactions in evaporitic settings, this study contributes to ongoing efforts to develop safe, science-based solutions for underground hydrogen storage in salt caverns.

1 Introduction and objectives

Hydrogen is widely recognised as a promising energy carrier for storing excess electricity generated from renewable sources and is expected to play a central role in the transition to a low-carbon energy system. A functioning hydrogen economy will require large-scale, long-duration storage solutions to balance variable – especially seasonal – supply and demand. However, major challenges remain, particularly in scaling up storage infrastructure and addressing the high production costs and energy inefficiencies of green and blue hydrogen. One proposed solution is Underground Hydrogen Storage (UHS), which involves injecting compressed hydrogen into deep geological formations (Abe et al., 2019; Tarkowski and Czapowski, 2018; Tarkowski, 2019; Iglauer et al., 2021).

The practice of underground gas storage in geological formations has long been implemented across various industrial sectors. These formations are common in many regions, offer

vast storage potential (IPCC, 2005; Lackner, 2003; Iglauer, 2022; Tarkowski et al., 2021) and, when topped with low-permeability caprock, are particularly effective at securely trapping gases such as natural gas, CO_2, CH_4, or H_2 (IPCC, 2005; Dake, 1978; Wollenweber et al., 2010; Nelson, 2009). Additionally, the cost associated with storing hydrogen in such geological formations (e.g., salt caverns, depleted hydrocarbon fields, aquifers) is generally projected to be lower than other industrial storage options like liquefied hydrogen or surface-compressed hydrogen storage (Sørensen, 2012) and provides much larger storage volumes (Matos et al., 2019).

Although hydrogen behaves similarly to natural gas in geological storage systems (Carden and Paterson, 1979; Lindblom, 1985), its lower molecular weight and higher diffusivity raise concerns about migration and containment (Panfilov et al., 2006). Moreover, hydrogen is more chemically reactive and susceptible to microbial consumption than natural gas, further complicating its geochemical behaviour. Among the various geological options available, salt formations have emerged as particularly favourable candidates for addressing many of these challenges.

Salt formations, particularly solution-mined salt caverns, are attractive for hydrogen storage due to their very low permeability, chemical inertness, and mechanical stability under pressure (Tarkowski and Czapowski, 2018; Foh et al., 1979). These features minimise the risk of leakage and geochemical alteration. The relatively low water content in salt caverns, compared to porous reservoir rocks, further minimizes the potential for unwanted side reactions, such as hydrogen hydroxide formation or infrastructure corrosion. Hydrogen storage in salt caverns has already been practised in industrial contexts – such as in Texas (USA), Teesside (UK), and Yakshunovskoe (Russia) – with little to no evidence of significant reactivity due to the inert nature of halite (Foh et al., 1979; Basniev et al., 2010). However, gas–rock interactions in such settings may involve dissolution–precipitation reactions among halite and impurities, potentially altering porosity, permeability, and cavern integrity (Bacci et al., 2011).

To evaluate the geochemical and physical stability of host rocks, laboratory experiments are commonly conducted to simulate subsurface conditions. These studies focus on potential changes in mineralogy, porosity, and permeability, and assess microbial activity under controlled thermodynamic conditions (Pichler, 2013; Bacci et al., 2011). Such experimental data are critical for assessing the feasibility, safety, and long-term performance of underground hydrogen storage projects (Berrezueta et al., 2024).

This study investigates the suitability of the Barbastro Formation, an Eocene evaporitic unit in the Southern Pyrenees (northeastern Spain), for hydrogen storage. Two rock salt samples from this formation were exposed to hydrogen gas under controlled laboratory conditions (10 MPa, 60 °C) for 30 d using a high-pressure autoclave. Pre- and post-exposure characterizations were performed using Scanning Electron Microscopy (SEM) and X-ray diffraction (XRD). The focus of this study was the assessment of mineralogical changes in the halite and other mineral phases, including anhydrite, silicates, and pyrite. While the results are specific to the conditions and scale of this study, they provide valuable insights into the geochemical stability and potential reactivity of salt formations during hydrogen exposure.

2 Geological background

The study area is situated within the northern margin of the Ebro Basin, the largest Cenozoic basin in the northeastern Iberian Peninsula (Fig. 1a). The Ebro Basin constitutes the southern foreland basin of the Pyrenees and is infilled with a thick and asymmetric Eocene to Pliocene sedimentary sequence (Riba et al., 1983) comprising marine to continental evaporitic and continental detrital sequences (Luzón, 2005). Zooming-in to the study area (Fig. 1b), it embraces the southern limb of the so-called Barbastro anticline (Gil and Jurado, 1998; Martínez-Peña and Pocoví, 1988; Pardo and Villena, 1979; Riba et al., 1983; Sans, 2003; Senz and Zamorano, 1992), an evaporitic-cored anticline that represents the western termination of the South Pyrenean Triangle Zone (e.g. Sans et al., 1996) and registers the latest and southernmost deformation of the Pyrenean orogeny in this area (e.g. Pocoví-Juan, 1978; Millán-Garrido et al., 2000). The southern limb involves the 60–70° south-dipping Peraltilla Fm. that becomes progressively horizontal from the core of the anticline to the south, and it is conformably covered by the Sariñena Fm. The core of the anticline is made of an intricate and laterally variable duplex system (Santolaria et al., 2020, 2024) involving the Barbastro Fm (Quirantes, 1978; Martínez-Peña and Pocoví, 1988). The duplex system is internally deformed, and characterized by gentle to isocline folds involving mudstone-dominated or gypsum-dominated levels respectively (García-Sansegundo and Teixell, 1990; Pardo and Villena, 1979). South of the anticline, this formation remains nearly undeformed (Fig. 1c).

Our study focuses on the evaporitic strata of the Barbastro Fm. This formation consists of late Priabonian to middle Rupelian (Gil and Jurado, 1998) alternating layers of sulphates, rock salt, and shales and subordinate red mudstones (Lucha et al., 2012; Luzón, 2005). In the subsurface, the Monzón-1 exploration well drilled an 886 m-thick unit of gypsum and marls with interbedded decameter-thick halite and anhydrite packages corresponding to this formation (Lanaja, 1987; Santolaria et al., 2020). Locally, this formation possibly exceeds 1000 m in thickness (García-Sansegundo and Teixell, 1990). It is interpreted as the product of "playa lake" environments, associated with the distal parts of alluvial fans, specifically the Salinar and Peralta Formations. The halite layers encountered in boreholes are interpreted as "salt pan" deposits, while the association of nodular gypsum, mudstones, and sandstones suggests sedimentation in a saline

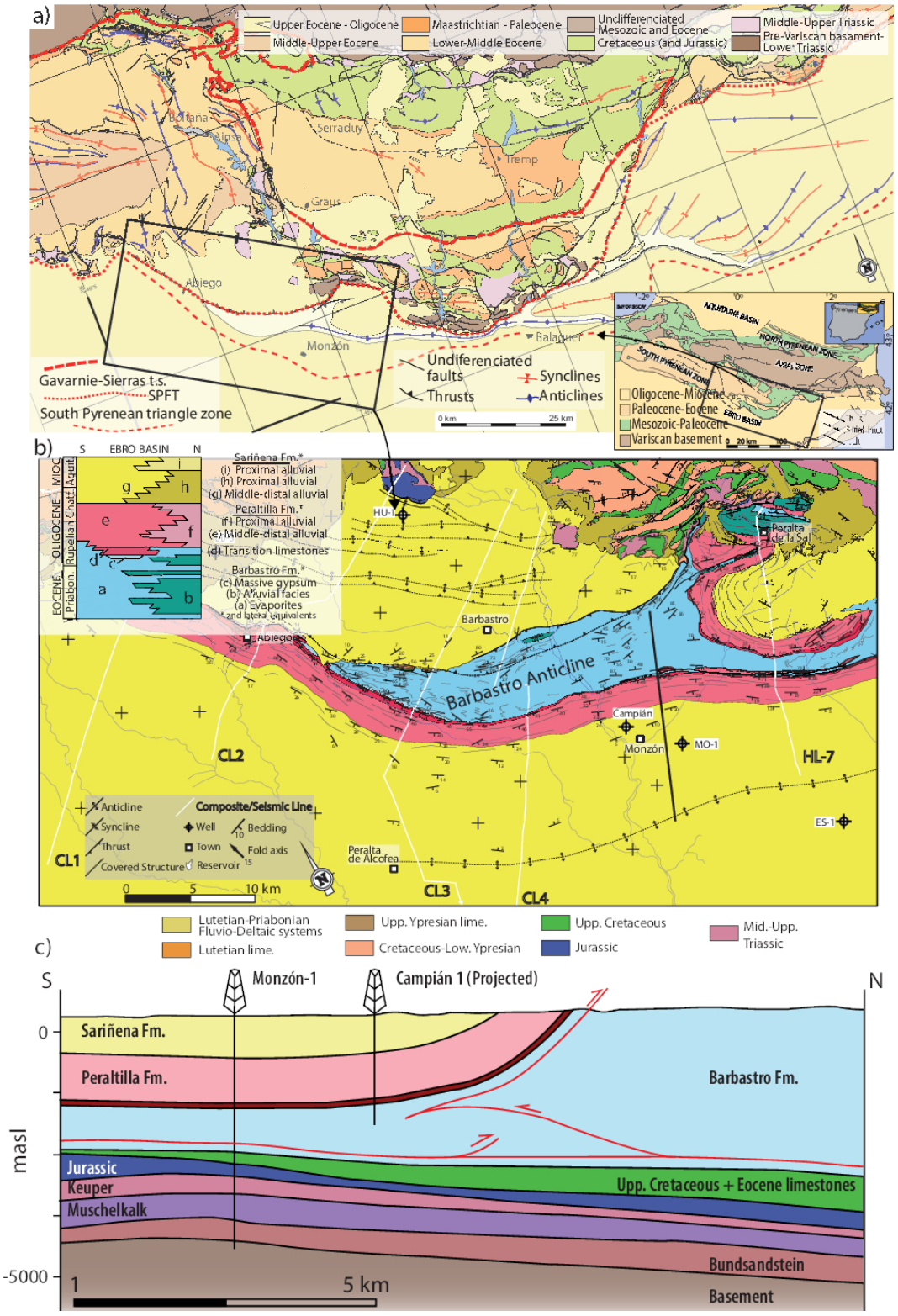

Figure 1. **(a)** Geological setting of the study area in the context of the Pyrenees. **(b)** Detailed geological cartography around the Barbastro anticline. Modified after Santolaria et al. (2020). **(c)** Geological cross-section across the Barbastro anticline integrating surface geological information (cartography and dip domains) with Monzón-1 (MO-1) and Campián-1 wells and the available seismic information. Location of the cross-section is shown in **(b)** with a NNW–SSE black line.

mudflat (continental sabkha) environment (García-Senz et al., 1991). This formation is of commercial interest due to its significant rock salt content, which was investigated through a deep borehole (Campián-1) drilled in 2018. The Campián-1 borehole intersected the Barbastro Fm. at a depth of approximately 1350 m (Fig. 1c; Soler-Sampere et al., 2021) and provided core samples for the experimental work presented in this study. This layered evaporitic sequence of the Barbastro Fm. is topped by the fluvial conglomerates, sandstones and mudstones of the Peraltilla and the Sariñena Fms (Lower to Upper Oligocene and Upper Oligocene to Lower Miocene, respectively). Exploration wells around and in the study area reveal that this Cenozoic succession overlies a Triassic to Lower Eocene sequence (Fig. 1c).

3 Materials and methods

3.1 Methods

From the methodological point of view, the study can be divided into three stages: (i) initial sample characterization; (ii) exposure to hydrogen gas under reservoir conditions; and (iii) post-exposure comparative studies.

Sample characterization was mostly based on microscopic techniques complemented by X-ray diffraction. The textural and mineralogical properties were studied with a Leica DM 6000 M optical microscope (OpM) at the Oviedo Unit of the CN-IGME (CSIC). The mineralogical composition was determined by X-ray diffraction using a Panalytical X'pert PRO MPD, with X'Celerator detector. Mineral identification was carried out with HighScore 3.0.4 software (PANalytical) using the PDF-2 (ICDD) and CODJanuary2021 Data Bases.

After sample preparation, selected rock salt specimens were oven-dried during 24 h at 40 °C to remove free water and minimize initial moisture content. Once dry, specific areas were analysed using a JEOL JSM-6010 LA PLUS Scanning Electron Microscope equipped with a tungsten filament, backscattered electron detector and EDS (dispersive energy X-ray) microanalysis, using low vacuum conditions. A total of 17 reference areas were selected (10 from sample CI-A and 7 from CI-C) each covering approximately 1 mm^2 to capture baseline microstructural and mineralogical features. These areas were documented at various magnifications for comparative analysis. Following SEM characterization, the samples were stored under ambient atmospheric conditions until their exposure to hydrogen gas. Both SEM and XRD analyses were conducted at the Central Laboratories of the IGME (Tres Cantos, Spain).

The samples were subsequently placed in an autoclave and exposed to hydrogen for 30 d at the Centro Nacional del Hidrógeno (Spain). No brine or other fluids were introduced into the reactor chamber. The experimental setup involves three T316 stainless steel reactors (Parr Instrument Company) with a capacity of 1 L (Fig. 2). Each reactor is equipped with: pressure indicator, pressure transmitter, thermocouple, gas inlet, gas outlet, 50 mL sampler and rupture disc set at 131 bar. Impurities inside the autoclave are removed, prior to H_2 injection, using N_2 as an inert gas. To keep the temperature constant at 60 °C, water is recirculated through the reactor jacket. The experiments were carried out at 100 bar. The test conditions were selected to simulate realistic subsurface reservoir environments.

Following hydrogen exposure, selected subsamples were analysed by X-ray diffraction to assess possible mineralogical changes. The same reference areas previously studied by SEM were re-examined under identical imaging conditions to detect microstructural or mineralogical alterations. The sequence of SEM analysis of the sample areas – comparing unexposed and exposed conditions – follows the protocol established in previous studies on rock–gas interactions (e.g., Berrezueta et al., 2024 and Ordóñez et al., 2024).

3.2 Materials

Core samples from a deep borehole were used in this study. The Campián-1 bis borehole perforates the evaporitic Barbastro Formation from 1357 m to the bottom of the hole at 1548.66 m (Soler-Sampere et al., 2021) (For further details see Sect. 2). Two relatively pure salt levels, CI-A at 1531.95 m and and CI-C at 1532.15 m depth, were selected for this study, and appropriate samples were prepared for the subsequent characterization and experimentation.

4 Results and discussion

4.1 Sample characterization

The two studied samples (CI-A and CI-C) are predominantly composed of halite (92 % and 99 %, respectively) of white-grey colour (Fig. 3a, b). The coarse-grained mosaic of halite spar consists of > 1 cm clean, subhedral crystals of polygonal-interlobate shape. Some halite crystals include high amounts of oriented fluid inclusions. At grain boundaries, small euhedral anhydrite crystals and other insoluble phases are common (Fig. 3c, d). In certain areas of the samples, the proportion of insoluble phases increase up to 70 %. These phases include anhydrite, quartz, feldspars, dolomite, calcite, phyllosilicates and pyrite. Among the phyllosilicate phases muscovite, illite, and clinochlore are the most prominent. Anhydrite is present either as a very fine-grained sulphate-silicate matrix or as prismatic-acicular crystals of up to 200 µm in size (Fig. 3e, f).

4.2 Exposure to hydrogen gas and comparative analyses

Following exposure to hydrogen, no macroscopically visible changes were observed in the samples. XRD analyses revealed no significant mineralogical alterations. However,

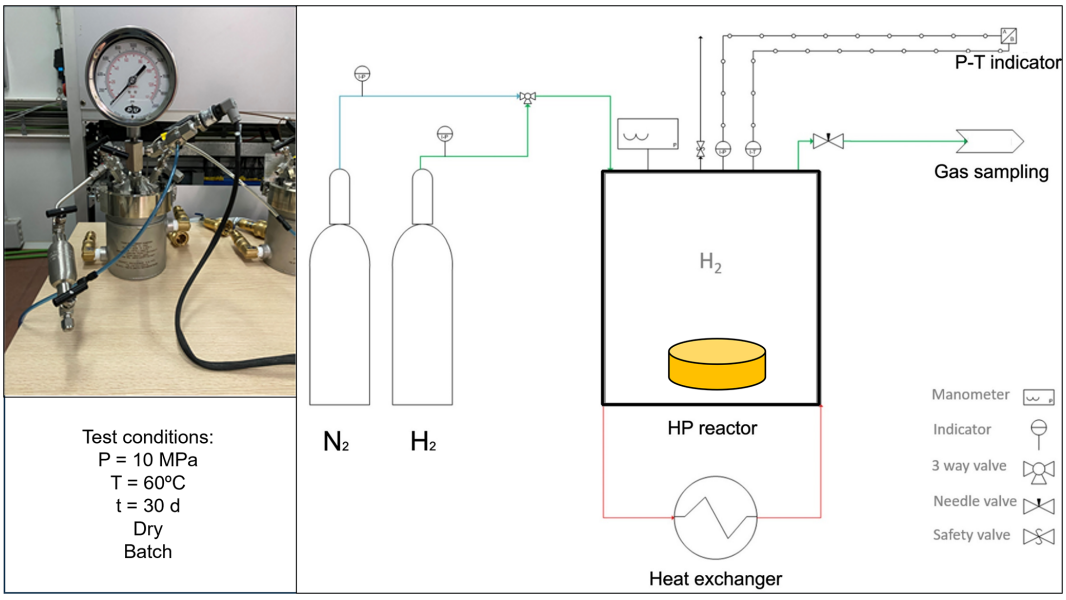

Figure 2. Configuration of the experimental setup. High-pressure stainless-steel reactor with temperature control.

SEM analysis of pre-selected reference areas showed minor but consistent microstructural changes, including: (i) particle detachment, (ii) halite recrystallization, and (iii) occasional formation of new mineral phases.

4.2.1 Particle detachment

The detachment and displacement of loose particles was the most frequently observed effect of hydrogen exposure (e.g., Fig. 4a–a′ and 4b–b′). These particles were predominantly anhydrite crystals, though aggregates of clay minerals and other insoluble phases were also occasionally displaced. In some cases, particle detachment appeared to result from the mechanical disintegration of individual mineral grains.

No chemical or mineralogical alterations were detected in the silicate, sulphate, or carbonate phases or in the pyrite and similar effects have frequently been observed by the authors in autoclave experiments using both reactive and inert gases (i.e., CO_2 and N_2) (e.g., Ordóñez et al., 2024). Therefore, we interpret this phenomenon as a purely physical effect, likely induced by pressurization and depressurization cycles during the experiment.

4.2.2 Halite recrystallization

Minor, but significant textural changes were observed in the halite after hydrogen exposure. Recrystallization processes led to a noticeable evolution in crystal morphology, characterised by the smoothing of previously well-defined crystallographic features. As a result, some pores were partially or entirely sealed (Fig. 4b–b′). Dispersed halite was observed to recrystallise into larger, subhedral crystals measuring 10–15 µm in diameter (Fig. 4c–c′). While the overall chemical composition of halite remained unchanged, the development of these textures indicates physical reorganization processes such as fluid-assisted diffusive mass transfer or grain boundary migration.

In surface energy–driven diffusion, halite dissolves from high-energy regions; the dissolved ions are transported via diffusion through brine layers coating grain surfaces and reprecipitate in pore spaces or at crack tips (Zeng et al., 2024). Another relevant mechanism is healing via recrystallization driven by grain boundary migration, in which the migrating boundary overgrows a fluid-filled crack, leaving behind isolated fluid inclusions (Houben et al., 2013).

Such microstructural transformations are commonly attributed to mechanisms that operate in the presence of water. Even under sub-saturated conditions, thin adsorbed water films may support measurable mass transfer, with diffusion coefficients estimated to range between 1×10^{-14} and 1×10^{-9} m^2 s^{-1}, depending on local humidity and film thickness (Koelemeijer et al., 2012). Although our experiment was conducted under nominally dry conditions, residual pore water, adsorbed atmospheric moisture, or fluid inclusions within the halite released by stress (Cyran et al., 2023) likely provided sufficient water activity to permit recrystallization. As mentioned in the Methodology section, the samples were stored under atmospheric conditions for several days before their exposure to H_2. The average RH in that period was around 80 % in the laboratory, which is above the deliquescence point of halite (75 % RH); therefore, water adsorption from the atmosphere is a plausible source of humidity content in the samples.

Our results demonstrate that even minimal water availability can trigger halite recrystallization under reservoir-like

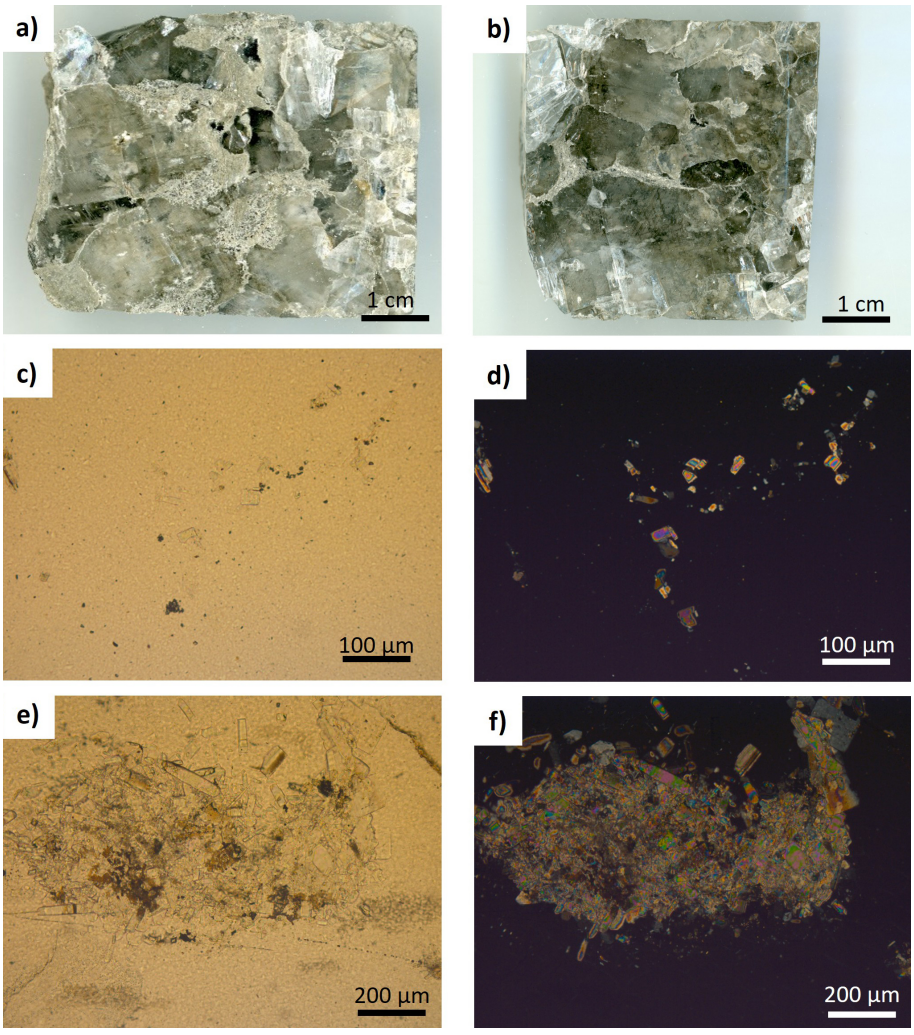

Figure 3. The studied rock salt samples: CI-A **(a)** and CI-C **(b)**. OpM photographs of texture and mineralogy. **(c, d)** Pure halite phase with $\leq 20\,\mu m$ anhydrite crystals accumulated around grain boundaries. **(e, f)** Anhydrite nodule with phyllosilicates, surrounded by halite. **(c, e)** Plain-polarised light; **(d, f)** cross-polarised light.

conditions, with observable microstructural changes developing over a relatively short experimental duration of 30 d.

It is worth noting that similar morphological changes in halite were observed by the authors during comparable autoclave experiments using N_2 gas (Mediato et al., 2025), suggesting that such features may not be unique to hydrogen exposure. Dedicated control tests under identical conditions but with inert gases (e.g., N_2 or Ar) would be useful to definitively separate the effects of gas composition from those of the experimental setup.

4.2.3 Formation of new mineral phases

In two of the observed reference areas of Sample CI-A, fine-grained ($< 10\,\mu m$), subhedral to euhedral chloride crystals were identified following hydrogen exposure (Fig. 5). Energy-dispersive X-ray spectroscopy (EDS) analysis revealed two distinct compositional types among these newly formed phases: the whitish crystals contained approximately 30 wt % potassium, while the darker grey crystals showed approximately 3 wt % of potassium and 7 wt % of magnesium. In all cases, sodium content was approximately 20 wt %; however, due to the halite matrix, this value might partly reflect background signal rather than incorporation into the new phases. All above values are semi-quantitative due to the analytical method.

Since these crystals were absent before the hydrogen exposure, we infer that they precipitated during the experiment as a result of partial halite dissolution followed by reprecipitation in the presence of potassium and magnesium ions. At the experimental conditions (10 MPa, 60 °C), the formation of sylvite (KCl), carnallite ($KMgCl_3 \cdot 6H_2O$), or intermediate phases within the KCl–$MgCl_2$–H_2O ternary system is ther-

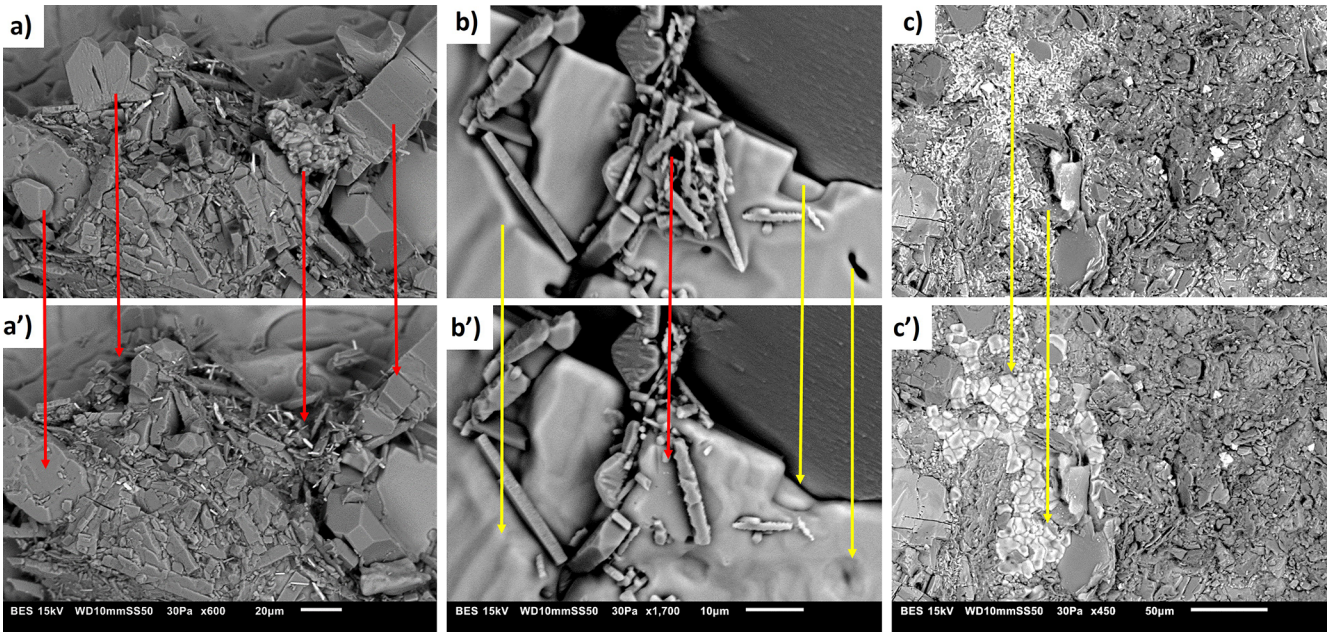

Figure 4. Examples of particle detachment (red arrows) (**a**–**a′**, **b**–**b′**) and halite recrystallization (yellow arrows) (**b**–**b′**, **c**–**c′**) (SEM images).

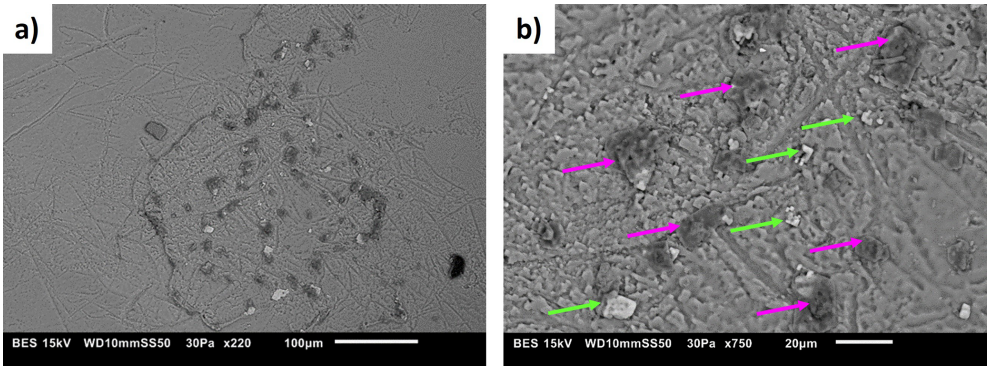

Figure 5. Newly formed chloride crystals (SEM images). Whitish minerals (green arrows) contain up to 35 wt % potassium, darker grey minerals (purple arrows) show an average of 2.5 wt % potassium and 7 wt % magnesium (EDS analysis).

modynamically plausible, depending on local ion concentrations (Yu et al., 2011).

The presence of both potassium- and magnesium-rich chloride phases in our samples suggests local supersaturation and favourable conditions for their nucleation. The source of these secondary cations remains uncertain; however, the dissolution or ion exchange processes involving clay minerals such as illite and chlorite (chlinochlore) present in the samples are considered the most probable contributors. Nonetheless, we observed no clear microstructural or chemical evidence for the degradation of these clay phases.

Therefore, while the formation of these chloride minerals suggests some degree of mobilization and redistribution of minor elements within the salt matrix, the precise mechanisms underlying their genesis – particularly the interaction between residual pore water, mineral surfaces, and hydrogen – remain to be clarified.

5 Conclusions

The results of this preliminary laboratory study support the potential feasibility of using salt caverns in the Barbastro Formation for hydrogen storage. Key findings include:

- The autoclave-based experimental setup successfully simulated subsurface storage conditions (60 °C, 10 MPa) over a 30 d period.
- No significant geochemical reactions or mineralogical alterations between rock and gas were observed in the sulphate, silicate, or carbonate phases.

- Halite underwent localized recrystallization, likely facilitated by trace amounts of water (e.g., residual pore water, adsorbed moisture, or fluid inclusions).
- New chloride phases were identified, though their formation mechanisms remain unclear and require further investigation.

These outcomes suggest that, under the tested conditions and at the tested scale, the salt matrix and associated impurity phases exhibit sufficient overall mineralogical stability for hydrogen storage applications. The observed microstructural changes – such as localized halite recrystallization, chloride precipitation and particle detachment – were minor and are likely related to pressure and temperature effects rather than specific interactions with hydrogen. Future studies should include tests with inert gases such as N_2 or Ar under identical conditions to isolate the influence of gas composition. Long-term experiments with cyclic exposure will also be critical to assess the operational stability of salt formations used in hydrogen storage.

Data availability. All used data are included in the article.

Author contributions. Conceptualization: TK, JM, JSG, JG, PMC, EB; Investigation: TK, BO, NG-M, PS, PC; Methodology: TK, BO, EB; Project administration: JM, JSG, JG; Writing (original draft preparation); TK, EB, PS, PC, NG-M; Writing: (review and editing): TK, JM, SR.

Competing interests. The contact author has declared that none of the authors has any competing interests.

Disclaimer. Publisher's note: Copernicus Publications remains neutral with regard to jurisdictional claims made in the text, published maps, institutional affiliations, or any other geographical representation in this paper. While Copernicus Publications makes every effort to include appropriate place names, the final responsibility lies with the authors. Also, please note that this paper has not received English language copy-editing. Views expressed in the text are those of the authors and do not necessarily reflect the views of the publisher.

Special issue statement. This article is part of the special issue "European Geosciences Union General Assembly 2025, EGU Division Energy, Resources & Environment (ERE)". It is a result of the EGU General Assembly 2025, Vienna, Austria & Online, 27 April–2 May 2025.

Acknowledgements. Thanks are due to the whole SMILE Team for their collaboration and to the two reviewers for their constructive comments.

Financial support. This research has been supported by the Centro para el Desarrollo Tecnológico Industrial (Project UES365).

The article processing charges for this open-access publication were covered by the CSIC Open Access Publication Support Initiative through its Unit of Information Resources for Research (URICI).

Review statement. This paper was edited by Johannes Miocic and reviewed by Juan Alcalde and Johannes Miocic.

References

Abe, J. O., Popoola, A. P. I., Ajenifuja, E., and Popoola, O. M.: Hydrogen energy, economy and storage: Review and recommendation, Int. J. Hydrogen Energy, 44, 15072–15086, 2019.

Bacci, G., Korre, A., and Durucan, S.: An Experimental and Numerical Investigation into the Impact of Dissolution/Precipitation Mechanisms on CO_2 Injectivity in the Wellbore and Far Field Regions, Int. J. Greenh. Gas Control, 5, 579–588, https://doi.org/10.1016/j.ijggc.2010.05.007, 2011.

Basniev, F. A., Omelchenko, K. S., and Adzynova, R. J.: Underground Hydrogen Storage Problems in Russia, in: 18th World Hydrogen Energy Conf. (WHEC 2010), Essen, Germany, 16–21 May 2010, edited by: Stolten, D. and Grube, T., 47–53, ISBN 978-3-89336-654-5, 2010.

Berrezueta, E., Kovács, T., Herrera-Franco, G., Caicedo-Potosí, J., Jaya-Montalvo, M., Ordóñez-Casado, B., Carrión-Mero, P., and Carneiro, J.: Laboratory Studies on Underground H2 Storage: Bibliometric Analysis and Review of Current Knowledge, Appl. Sci., 14, 11286, https://doi.org/10.3390/app142311286, 2024.

Carden, P. and Paterson, L.: Physical, Chemical and Energy Aspects of Underground Hydrogen Storage, Int. J. Hydrogen Energy, 4, 559–569, https://doi.org/10.1016/0360-3199(79)90083-1, 1979.

Cyran, K., Toboła, T., and Kamiński, P.: Experimental study on mechanically driven migration of fluids in rock salt, Engineering Geology, 313, 106975, https://doi.org/10.1016/j.enggeo.2022.106975, 2023.

Dake, L. P.: Fundamentals of Reservoir Engineering, 1st edn., Elsevier, Amsterdam, ISBN 978-0-444-41830-2, 1978.

Foh, S., Novil, M., Rockar, E., and Randolph, P.: Underground Hydrogen Storage. Final Report [Salt Caverns, Excavated Caverns, Aquifers and Depleted Fields], Brookhaven National Laboratory, Upton, NY, https://doi.org/10.2172/6536941, 1979.

García-Sansegundo, J. and Teixell Cácharo, A.: Mapa Geológico de España 1 : 50.000, Hoja No. 287 (Barbastro) y Memoria, IGME, Spain, ISBN 978-84-7840-946-4, 1990.

García-Senz, J., Zamorano-Cáceres, M., Montes, M. J., and Rico, M.: Mapa Geológico de España 1 : 50.000, Hoja No. 326 (Monzón) y Memoria, IGME, Spain, ISBN 978-84-9138-039-9, 1991.

Gil, J. A. and Jurado, M. J.: Geological Interpretation and Numerical Modelling of Salt Movement in the Barbastro–Balaguer Anticline, Southern Pyrenees, Tectonophysics, 293, 3–4, https://doi.org/10.1016/S0040-1951(98)00097-3, 1998.

Houben, M. E., ten Hove, A., Peach, C. J., and Spiers, C. J.: Crack Healing in Rocksalt via Diffusion in Adsorbed Aqueous Films:

Microphysical Modelling Versus Experiments, Phys. Chem. Earth, 64, 95–104, https://doi.org/10.1016/j.pce.2012.10.001, 2013.

Iglauer, S.: Optimum Geological Storage Depths for Structural H2 Geo-Storage, J. Pet. Sci. Eng., 212, 109498, https://doi.org/10.1016/j.petrol.2021.109498, 2022.

Iglauer, S., Abid, H., Al-Yaseri, A., and Keshavarz, A.: Hydrogen Adsorption on Sub-Bituminous Coal: Implications for Hydrogen Geo-Storage, Geophys. Res. Lett., 48, https://doi.org/10.1029/2021GL092976, 2021.

IPCC: Special Report on Carbon Dioxide Capture and Storage, Working Group III of the Intergovernmental Panel on Climate Change, Cambridge University Press, Cambridge, UK and New York, NY, USA, ISBN 978-0-521-68551-1, 2005.

Koelemeijer, P. J., Peach, C. J., and Spiers, C. J.: Surface Diffusivity of Cleaved NaCl Crystals as a Function of Humidity: Impedance Spectroscopy Measurements and Implications for Crack Healing in Rock Salt, J. Geophys. Res., 117, B01205, https://doi.org/10.1029/2011JB008627, 2012.

Lackner, K. S.: A Guide to CO_2 Sequestration, Science, 300, 1677–1678, https://doi.org/10.1126/science.1079033, 2003.

Lanaja, J. M.: Contribución de la exploración petrolífera al conocimiento de la Geología de España (Inst. Geol. Mine. España Ed.), 465 pp., 17 mapas, ISBN 978-84-7474-398-2, 1987.

Lindblom, U.: A Conceptual Design for Compressed Hydrogen Storage in Mined Caverns, Int. J. Hydrogen Energy, 10, 667–675, https://doi.org/10.1016/0360-3199(85)90006-0, 1985.

Lucha, P., Gutiérrez, F., Galve, J. P., and Guerrero, J.: Geomorphic and stratigraphic evidence of incision-induced halokinetic uplift and dissolution subsidence in transverse drainages crossing the evaporite-cored Barbastro-Balaguer anticline (Ebro Basin, NE Spain), Geomorphology, 171–172, 154–172, https://doi.org/10.1016/j.geomorph.2012.05.015, 2012.

Luzón, A.: Oligocene–Miocene alluvial sedimentation in the northern Ebro Basin, NE Spain: Tectonic control and palaeogeographical evolution. Sedimentary Geology, 177, 19–39, 2005.

Martínez-Peña, B. and Pocoví, A.: El amortiguamiento frontal de la estructura de la cobertera surpirenaica y su relación con el anticlinal de Barbastro-Balaguer, Acta Geológica Hispánica, 23, 81–94, 1988.

Matos, C. R., Carneiro, J. F., and Silva, P. P.: Overview of Large-Scale Underground Energy Storage Technologies for Integration of Renewable Energies and Criteria for Reservoir Identification, J. Energy Storage, 21, 241–258, https://doi.org/10.1016/j.est.2018.11.023, 2019.

Mediato, J., Ordóñez, B., and Berrezueta, E.: Estudios químicos, mineralógicos y texturales de alteraciones de superficies minerales expuestas al gas hidrógeno bajo condiciones de reservorio, unpublished project report, H2SALT Project, https://www.h2saltproject.com (last access: 25 September 2025), 2025.

Millán-Garrido, H., Pueyo, E., Aurell, M., Luzón, A., Oliva-Urcia, B., Martínez-Peña, M. B., and Pocoví Juan, A.: Actividad tectónica registrada en los depósitos terciarios del frente meridional del Pirineo central, Revista Sociedad Geológica España, 13, 279–300, 2000.

Nelson, P. H.: Pore-Throat Sizes in Sandstones, Tight Sandstones, and Shales, Am. Assoc. Pet. Geol. Bull., 93, 329–340, https://doi.org/10.1306/10240808059, 2009.

Ordóñez, B., Mediato, J., Kovacs, T., Martínez-Martínez, J., Fernández-Canteli, P., González-Menéndez, L., Roces, S., Caicedo-Potosí, J., del Moral, B., and Berrezueta, E.: Experimental geochemical assessment of a seal-reservoir system exposed to supercritical CO_2: A case study from the Ebro Basin, Spain, Int. J. Greenh. Gas Control, 137, 104233, https://doi.org/10.1016/j.ijggc.2024.104233, 2024.

Panfilov, M., Gravier, G., and Fillacier, S.: Underground Storage of H_2 and H_2–CO_2–CH_4 Mixtures, in: Proc. ECMOR-X – 10th European Conference on the Mathematics of Oil Recovery, Amsterdam, The Netherlands, 4–7 September 2006, cp-23-00003, https://doi.org/10.3997/2214-4609.201402474, 2006.

Pardo, G. and Villena-Morales, J.: Aportación a la geología de la región de Barbastro, Acta geológica hispánica, ISSN 0567-7505, 289–292, 1979.

Pichler, M.: Assessment of Hydrogen–Rock Interactions During Geological Storage of CH_4–H_2 Mixtures, MSc thesis, unpublished, Montanuniversität Leoben, Austria, https://www.underground-sun-storage.at/fileadmin/bilder/tx_templavoila/Final_Version_Master_Thesis_Markus_Pichler_about_Storage_of_H2-CH4_Mixtures_in_the_Underground_06.pdf (last access: 25 September 2025), 2013.

Pocoví-Juan, A: Estudio geológico de las sierras Marginales Catalanas (Prepirineo de Lérida), Acta Geológica Hispánica, 73–79, 1978.

Quirantes, J.: Estudio sedimentológico y estratigráfico del Terciario Continental de los Monegros, Instituto Fernando el Católico, (CSIC), Diputación Provincial de Zaragoza, Publicación 681, 1978.

Riba, O., Reguant, S., and Villena, J.: Ensayo de síntesis estratigráfica y evolutiva de la Cuenca terciaria del Ebro, in: Libro Jubilar, edited by: Ríos, J. M., Geología de España, Tomo II, Instituto Geológico y Minero de España, 131–159, ISBN 9788474743876, 1983.

Sans, M.: From thrust tectonics to diapirism. The role of evaporites in the kinematic evolution of the eastern South Pyrenean front, Geologica Acta, 1, 239–259, 2003.

Sans, M., Muñoz, J. A., and Vergés, J.: Triangle zone and thrust wedge geometries related to evaporitic horizons (southern Pyrenees), Bulletin of Canadian Petroleum Geology, 44, 375–384, 1996.

Santolaria, P., Ayala, C., Pueyo, E. L., Rubio, F. M., Soto, R., Calvín, P., Luzón, A., Rodríguez-Pintó, A., Oliván, C., and Casas-Sainz, A. M.: Structural and geophysical characterization of the western termination of the South Pyrenean triangle zone, Tectonics, 39, e2019TC005891, https://doi.org/10.1029/2019TC005891, 2020.

Santolaria, P., Ayala, C., Soto, R., Clariana, P., Rubio, F. M., Martín-León, J., Pueyo, E. L., and Muñoz, J. A.: Salt distribution in the South Pyrenean Central Salient: Insights from gravity anomalies, Tectonics, 43, e2024TC008274, https://doi.org/10.1029/2024TC008274, 2024.

Senz, J. G. and Zamorano, M.: Evolución tectónica y sedimentaria durante el Priaboniense superior-Mioceno inferior, en el frente de cabalgamiento de las Sierras Marginales occidentales, Acta geológica hispánica, 27, 195–209, 1992.

Soler-Sampere, M., García-Senz, J., Salazar, A., Mata, M. P., and González Blázquez, J.: Nuevos Datos del Relleno Sedimentario del Borde Norte de la Cuenca del Ebro Aportados por la Testifi-

ción Continua del Sondeo Campián-1 Bis (Monzón, Huesca), in: X Congreso Geológico de España, 6–8 June 2021, Vitoria-Gasteiz, Spain, Geotemas (Madrid), 18, 1134, ISSN 1576-5172, 2021.

Sørensen, B.: Chapter 6 – Social Implications In Sustainable World, Hydrogen and Fuel Cells, 2nd Edn., Academic Press, 361–402, ISBN 9780123877093, https://doi.org/10.1016/B978-0-12-387709-3.50006-1, 2012.

Tarkowski, R.: Underground Hydrogen Storage: Characteristics and Prospects, Renew. Sustain. Energy Rev., 105, 86–94, https://doi.org/10.1016/j.rser.2019.01.051, 2019.

Tarkowski, R. and Czapowski, G.: Salt Domes in Poland – Potential Sites for Hydrogen Storage in Caverns, Int. J. Hydrogen Energy, 43, 21414–21427, https://doi.org/10.1016/j.ijhydene.2018.09.212, 2018.

Tarkowski, R., Uliasz-Misiak, B., and Tarkowski, P.: Storage of Hydrogen, Natural Gas, and Carbon Dioxide – Geological and Legal Conditions, Int. J. Hydrogen Energy, 46, 20010–20022, https://doi.org/10.1016/j.ijhydene.2021.03.131, 2021.

Wollenweber, J., Alles, S., Busch, A., Krooss, B. M., Stanjek, H., and Littke, R.: Experimental Investigation of the CO_2 Sealing Efficiency of Caprocks, Int. J. Greenh. Gas Control, 4, 231–241, https://doi.org/10.1016/j.ijggc.2010.01.003, 2010.

Yu, X., Zeng, Y., Yao, H., and Yang, J.: Metastable Phase Equilibria in the Aqueous Ternary Systems $KCl + MgCl_2 + H_2O$ and $KCl + RbCl + H_2O$ at 298.15 K, J. Chem. Eng. Data, 56, 8, 3384–3391, https://doi.org/10.1021/je200360f, 2011.

Zeng, Z., Ma, H., Yang, C., Zhao, K., Liang, X., Li, H., and Zheng, Z.: Self-Healing Behaviors of Damaged Rock Salt Under Humidity Cycling, Int. J. Rock Mech. Min. Sci., 174, 105636, https://doi.org/10.1016/j.ijrmms.2024.105636, 2024.